

## Chapter 2

# Fundamental Operations of Bone Machining

Currently, the majority of conventional orthopedic surgeries adopted for shaping and forming bones involve the contact methods based on controlled mechanical fracturing (chipping) of the bones. The fundamental operations involved in mechanical fracturing of bone are drilling, sawing, grinding/abrasive machining, and milling. The various methods designed for mechanically shaping and forming bones during orthopedic surgeries in the clinical environment are either based on single or combinations of these fundamental operations. The examples of methods based on combinatorial fundamental operations are: ultrasonic, pneumatic, and hydraulic machining. In addition to these mechanical operations/methods, several non-contact thermal photon/electron energy based techniques are also being researched for their possible use in orthopedic surgeries. The thermal energy-(bone) material interaction raises its temperature to the melting or vaporization temperature depending upon the magnitude of the thermal energy and photon/electron energy-material interaction characteristics. Thus a bone can be shaped and formed by removal of the bone material through controlled melting and/or vaporization. The non-contact thermal machining techniques/methods based on photonic/electron energy that are being explored in bone machining include but not limited to laser, microwave, and ion beam machining. The purpose of this chapter is to present only the fundamental principles behind mechanical and thermal operations in removal (machining) of material in general. Whereas, the implementation of these fundamental operations and methods/techniques particularly for machining of bones are described in detail in Chaps. 3, 4, and 5.

### 2.1 Drilling

Drilling is a basic machining operation to cut a hole into solid material. It can be further extended to enlarge previously drilled holes and in that case the operation can be described as core drilling or counter drilling/boring. If the same drill is employed to cut a hole of two or more diameters, the operation is termed as step drilling. For

enlarging the hole with an intention to achieve more accuracy, a boring operation is adopted. On the contrary, if the intentions are not just to enlarge a hole but also produce hole of accurate size and good surface finish with minimal material removal, an operation of reaming is employed. Furthermore, operations of enlarging a hole to a limited depth, enlarging a hole with a shallow depth to just finish face around the original hole, and cutting of an angular opening into the end of a hole are termed as counterboring, spot facing, and countersinking respectively. Finally, center drilling is an operation used to drill a hole that will act as a center of rotation for many other above mentioned drilling operations. Center drilling is typically performed using a drill with a special shape, known as a center drill.

These various drilling operations and the types of drills employed during these operations are schematically presented in Fig. 2.1. The most common type of drill used in drilling operation is the standard-point twist drill. They possess helical grooves or flutes as shown on the drill in Fig. 2.1. The geometric parameters (cutting lips and edges) that influence the drilling performance of a drill are a point angle, lip-relief angle, a chisel-edge angle, and a helix angle. These geometric parameters are schematically illustrated in Fig. 2.2 [1]. The helix angle varies from  $18^\circ$  to  $40^\circ$  for the drill used to drill hard materials and soft materials respectively. The cutting lip relief angle ranges between  $12\text{--}15^\circ$  at the outside diameter and decreases toward the axis of the drill whereas too much relief weakens the cutting edge and reduces drill life. Although the average point angle is  $118^\circ$  it can vary for specific purposes from  $136^\circ$  for hard materials (steels) to  $60^\circ$  for soft materials (wood). Maintaining equal length of the cutting edges or lips along with their orientation in equal angle with the axis of the drill are important for their accurate/precision performance over its long life time.

Typically drilling operation can be categorized in two major operating regimes as low speed and high speed operating conditions [2]. A low speed drilling involves tool wear largely by abrasion and interaction of surface asperities under high pressure leading to edge deterioration and formation and fracture of fusion zones. On the contrary, although at high speed drilling high temperature development contributes to drill wear, the material next to the drill face becomes weaker and shears more easily in friction while both the coefficient of friction and the friction force remain low. If

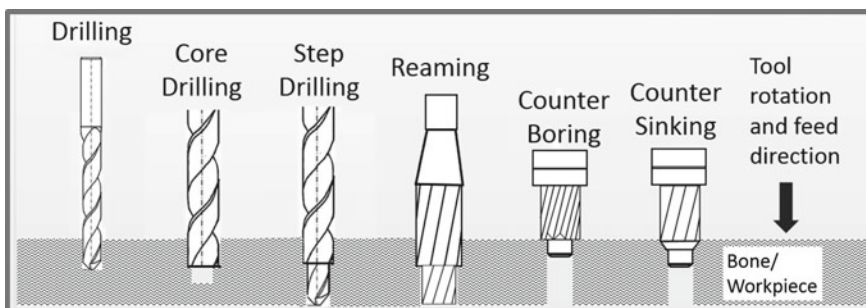


**Fig. 2.1** Various drilling operations

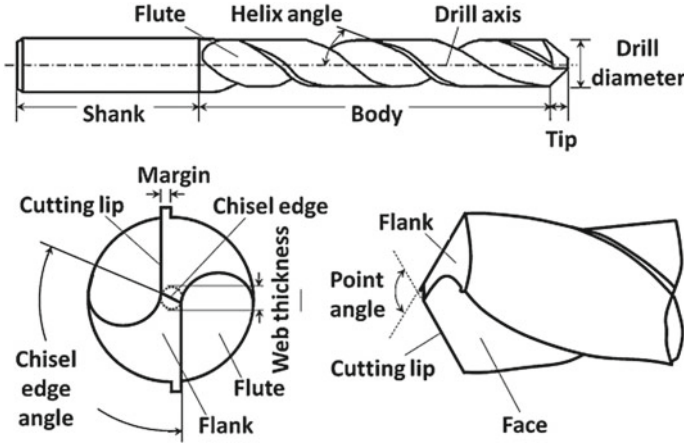


**Fig. 2.2** Geometric features of twist drill (reprinted from Lee et al. [1] with permission. © Elsevier)

the drill of rotational velocity  $V_d$  exerts a force  $F$  (the force applied to the drill) on the chip being removed from the workpiece (assuming orthogonal machining) and its resolution (drilling force) in the direction of drill velocity is  $F_d$  then power,  $P$  required to drill is

$$P = F_d V_d \quad (2.1)$$

The power does not increase linearly with speed as the drilling force decrease at increased speed. During drilling the force that acts in the direction of the hole axis is defined as the thrust force [2]. The thrust force depends upon various factors such as feed, rotational speed, drill diameter, drill geometry, and the strength of the workpiece material. The power,  $P$  dissipated during drilling is the product of torque and rotational velocity,  $V_d$ . The measurement and direct correlation of these parameters with thrust force is complex and difficult. However, the material removal rate in drilling  $MRR_{drill}$  can be expressed in the following simplistic relationship.

$$MRR_{drill} = \frac{\pi D^2}{4} f_d R \quad (2.2)$$

where  $D$  is the drill diameter,  $f_d$  is the feed per rotation and  $R$  is the rotational velocity.

## 2.2 Sawing

In sawing the cutting tool is a blade (saw) with series of small teeth on its periphery (edge) that remove a small amount of material by reciprocating linear or unidirectional linear or circular motion. In sawing, due to a narrow width of cut (kerf) small volume of material is removed (wasted). The important parameters associated with

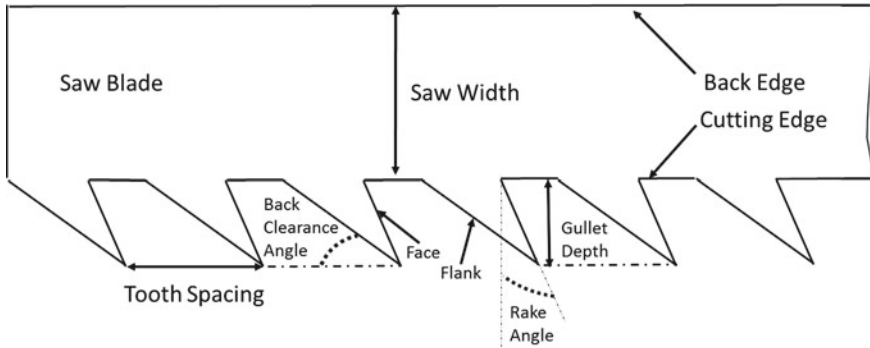


**Fig. 2.3** Various geometric features of a saw

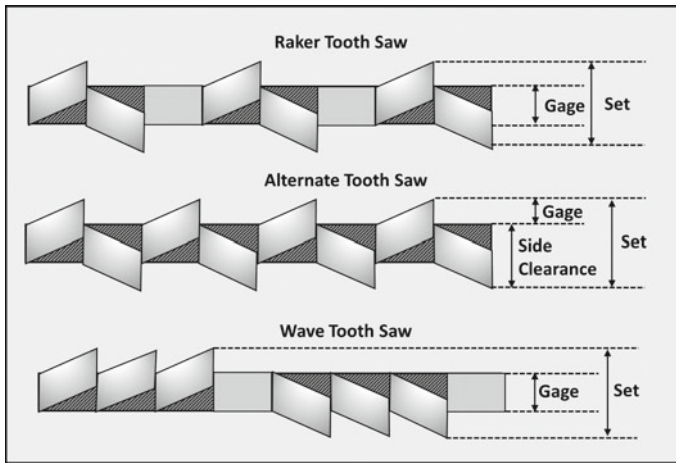
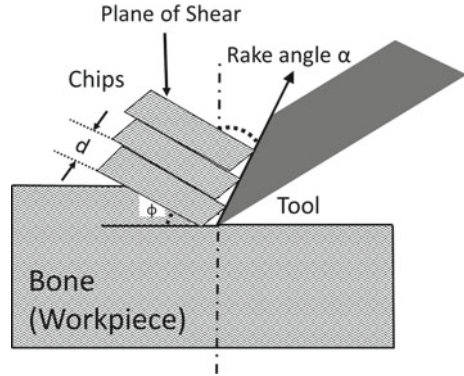


**Fig. 2.4** Types of saw teeth

a saw are (1) material, (2) tooth spacing (pitch), (3) tooth size, (4) tooth form, and (5) tooth set and these are schematically illustrated in Fig. 2.3 [2]. Low alloy, high-carbon steel, special steel alloy including stainless steel, and high speed steel are the preferred materials for saw. Often, the saw teeth tips are welded/fused/inserted with diamond, ferrous or non-ferrous carbide, and high speed steels for better performance and longer lifetime of the saw. The performance of a saw in terms of rate of volume of material removal and depth of cut are highly influenced by the pitch. Coarse teeth are suitable for wider and faster cut whereas fine teeth are appropriate for narrow cut. The pitch of circular saw is usually in the range of 5–51 mm and typically the straight saws are available with the teeth in the range of 2 teeth/in. to 32 teeth/inch. The rake angle and clearance angle corresponding to single-point tool along with alternate offsetting of the teeth with respect to the saw plane (Fig. 2.4) provide anti-binding and anti-rubbing characteristics to the saw during cutting [2].

**Fig. 2.5** Schematic of basic mechanism of chip formation during cutting



Even though the sawing blades have different shapes/forms (linear and circular) their series of cutting teeth operate in the same basic manner. Therefore, the principles of sawing (machining) operation can be explained on the basis of theory related to cutting by single-point cutting tool [2]. The basic mechanics of actual three dimensional sawing process can be simplistically explained by two dimensional orthogonal cutting model where the saw tooth edge is perpendicular to the movement of the saw (Fig. 2.5) [2].

As during sawing, the chips are generally produced by shearing process (Fig. 2.5) shearing occurs along a shear plane at the shear angle,  $\Phi$  with the surface of the workpiece. The orthogonal cutting includes a configuration of a rake angle,  $\alpha$ ; a relief or clearance angle and tool angle that together add to  $90^\circ$  (Fig. 2.5).

For a saw set up at a cutting (sawing) speed,  $V_s$  to remove an unformed workpiece layer of thickness,  $h_o$  and a chip of thickness,  $h_c$ , then the cutting ratio,  $R_c$  and the shear angle,  $\Phi$  are expressed as

$$R_c = \frac{h_o}{h_c} \text{ and } \tan \Phi = \frac{R_c \cos \alpha}{1 - R_c \sin \alpha} \quad (2.3)$$

Since chip thickness,  $h_c$ , is greater than the depth of unformed workpiece layer of thickness,  $h_o$ , the velocity of the chip,  $V_c$ , has to be less than the sawing speed,  $V_s$ , thereby maintaining the continuity of mass expressed by the following relationships.

$$V_s h_o = V_c h_c \text{ or } V_c = V_s R_c \text{ or } V_c = V_s \frac{\sin \Phi}{\cos(\Phi - \alpha)} \quad (2.4)$$

Finally, assuming an ideal condition where all shear during sawing is concentrated in an infinitely thin shear layer, the shear strain,  $\Gamma$  can be expressed as

$$\Gamma = \frac{V_s}{\cos(\Phi - \alpha)} = \frac{V_{shear}}{\cos \alpha} = \frac{V_c}{\sin \Phi} \quad (2.5)$$

where  $V_{shear}$  is the shearing velocity in shearing plane. For the sheared element (shear volume) of finite thickness,  $d$ , the shear strain,  $\Gamma$  can be expressed as

$$\Gamma = \frac{V_{shear}}{d} \quad (2.6)$$

The chip morphology significantly affects surface finish, integrity, and the overall sawing operation. The magnitude of the shear angle,  $\Phi$ , for given undeformed chip thickness controls the sawing force and energy.

## 2.3 Grinding/Abrasive Machining

Abrasive/grinding machining is a process of material removal via accelerated wear/fracture of a surface by a multitude of hard, angular hard abrasive particles or grains (grits) bonded or not bonded to a tool of definite form. The material removal can be small (fine) or large scale. Typically abrasive/grinding machining is the last operation performed on the component as often it is employed to produce high quality surface finish (roughness) with a desirable residual stress distribution and without surface and sub-surface damage along with close dimensional tolerance.

The grits or abrasives commonly used during abrasive/grinding machining can be broadly categorized as conventional (aluminum oxide and silicon carbide) and super (cubic boron nitride and diamond) abrasives [1–3]. The life time and performance of these grits are function of their various physical and geometric properties such hardness, toughness, resistance to attrition and fracture, friability, shape, and size. Hardness is the ability of the grit to resist penetration while abrading/scratching the workpiece surface. The greater difference in hardness between a grit and the workpiece will result in more effective and efficient grinding process. Super abrasives are the hardest materials. Toughness is body strength of a grit to withstand the mechanical shocks. Attrition and friability are the abilities of a grit to dull or deteriorate by fragmentation in fine particles and break/fracture into large pieces during grinding operation. Friability provides self-sharpening ability while resistance to attrition maintains sharpness of the grit/abrasive. Both attrition and friability of the grit depends upon hardness and toughness of the grit material to sharpen and maintain the sharpness of the grit during abrasive machining. Furthermore, friability is also dependent on the shape and size of the grit. While blocky grits are less friable compared to plate-like (flat) grits, the finer grits due to smaller probability of defects in them are stronger and less friable than larger grits.

Typically abrasive/grinding machining operations are carried out with abrasive/grinding wheels or rotary tools bonded with grits of various shapes and sizes into disks, cylinders, and cones of various shapes and sizes. The basic types of grinding/abrasive machining are surface, cylindrical, internal, and center-less grinding/abrasive machining [4]. Grinding of a flat surface is surface grinding; in cylindrical grinding (center type grinding), the external cylindrical surface and shoulder of the

workpiece are ground; in external grinding, a small diameter wheel grinds the inside diameter of the workpiece; and when the workpiece is ground by a grinding wheel or tool without supporting by centers or chucks, the process is termed as center-less grinding. These grinding/abrasive machining operations are schematically illustrated in Fig. 2.6.

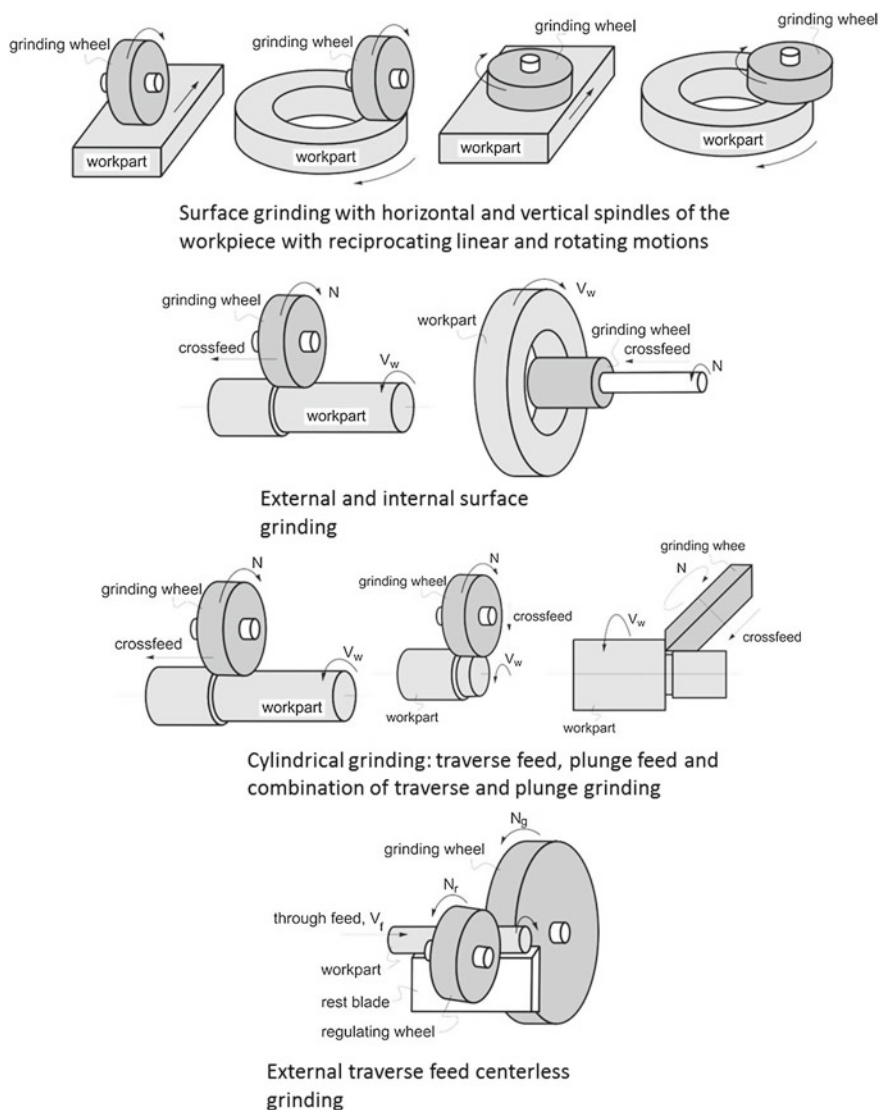


**Fig. 2.6** Types of grinding

The attributes of grinding/abrasive machining are expressed in various manners. The grinding ratio,  $G$  correlates the amount of material removed (ground) with the grinding wheel/tool wear by the following formula.

$$G = \frac{\text{Volume of material removed}}{\text{Volume of wheel material}} \quad (2.7)$$

The grinding ratio depends upon type of wheel, workpiece material, grinding/cooling fluid, depth of cut, and speed of wheel and workpiece. In surface grinding operation (Fig. 2.7) [2] the length,  $l$ , of undeformed portion of the workpiece in contact of the grinding wheel is approximately represented by the following relationship.

$$l \approx (Dd)^{\frac{1}{2}} \quad (2.8)$$

where  $D$  is the diameter of the wheel and  $d$  is the wheel depth of cut. Assuming  $v \ll V$  and width of the workpiece unity, the number of chips and the corresponding volume of the material removed per unit time are  $VC$  and  $vd$  respectively where  $V$ ,  $v$ , and  $C$  are the tangential velocity of the grain on the periphery of the wheel, velocity of the workpiece, and the number of cutting points per unit area of wheel surface respectively. Furthermore, assuming the chip removed is of constant width,  $w$ , and rectangular in the cross section, the volume of the chip,  $V_{chip}$ , is represented by the following formula.

$$V_{chip} = \frac{wtl}{2} \quad (2.9)$$

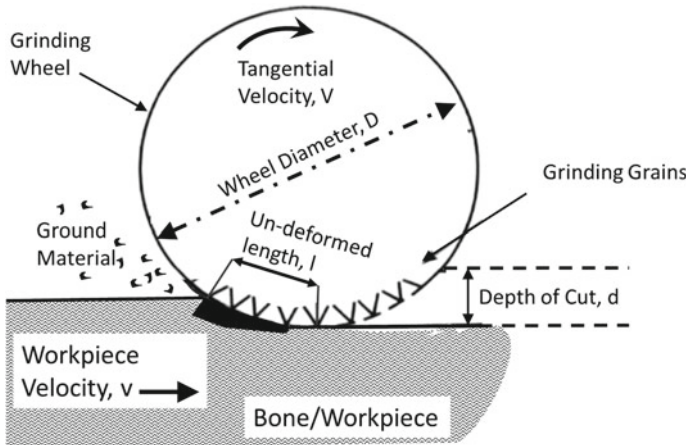


**Fig. 2.7** Surface grinding operation



where  $t$  is the grain depth of cut (undeformed portion of the workpiece in contact with the wheel). Next, the volume of material removed per unit time is given by the following relationship.

$$\text{Volume of workpiece material ground/time} = \frac{\text{Number of chips removed/time}}{\text{Volume of each chip}} \quad (2.10)$$

that is

$$vd = VC.V_{chip} = \frac{VCwtl}{2} \quad (2.11)$$

Finally,  $t$ , the thickness of undeformed portion of the workpiece in contact with the wheel that is eventually removed as a chip of average thickness  $X$ , is given by

$$t = \frac{2v^{\frac{1}{2}}X^{\frac{1}{2}}d^{\frac{1}{4}}}{V^{\frac{1}{2}}C^{\frac{1}{2}}w^{\frac{1}{2}}D^{\frac{1}{4}}} \quad (2.12)$$

As the accuracy of dimensions of the surface precision grinding/abrasive machining is affected by the force on the grit, the force is proportional to the cross sectional area of the undeformed portion of the workpiece in contact with the wheel, the relative grit force is presented by

$$\text{Relative grit force} \propto \frac{vd^{\frac{1}{2}}}{VCD^{\frac{1}{2}}} \quad (2.13)$$

Finally, the temperature developed during grinding/abrasive machining can have adverse effects such as development of thermal and residual stresses in the surface and subsurface regions thereby introducing dimensional distortions in the workpiece. The temperature rise in surface and subsurface region,  $\Delta T$ , is function of the total energy input to the surface area being ground and represented as

$$\Delta T \propto ud \quad (2.14)$$

where  $u$  is the specific energy consumed in producing a chip. If  $u$  is assumed to be varying inversely with the thickness of undeformed portion of the workpiece in contact with the wheel,  $t$ , then rise in temperature is given by

$$\Delta T \propto \frac{d}{t} \propto d^{\frac{3}{4}}V^{\frac{1}{2}}C^{\frac{1}{4}}D^{\frac{1}{4}}V^{\frac{1}{2}} \quad (2.15)$$

Although, localized temperatures at the wheel-workpiece contact region developed can be very high ( $>1000^{\circ}\text{C}$ ) and time of contact being very short, depending upon the type of the workpiece material melting may or may not occur during grinding/abrasive machining.

## 2.4 Milling

Milling is a versatile machining (material removal) operation capable of producing a wide range of machined (cut) geometries including flat surfaces, pockets, angles, contours, steps, and slots [1, 2]. The tools or milling cutter employed for each of these operations are different and specialized. These tools/cutters have multiple teeth cutting edges configured around an axis that produce number of chips per revolution. The machining action is generated by rotation of the tool and the feed by motion of the workpiece. The combination of type of tool/cutter and feed mechanism together define types of milling operations and resulting milling geometries as schematically depicted in Fig. 2.8 [5].

The efficiency of the milling process can be realized through various critical machining parameters such as cutting/milling speed,  $V_m$ ; feed per tooth,  $f_m$ ; milling time,  $t_m$ ; and material removal rate,  $MRR_{mill}$ . In milling, the cutting/milling speed,  $V_m$  is the peripheral speed of the tool/cutter and it is given by

$$V_m = \pi D_m N_m \quad (2.16)$$

where  $D_m$  is the cutter diameter and  $N_m$  is the rotational speed of the cutter as shown in Fig. 2.9. Feed per tooth,  $f_m$  and machine feed rate,  $V_m$  can be represented by the following equations.

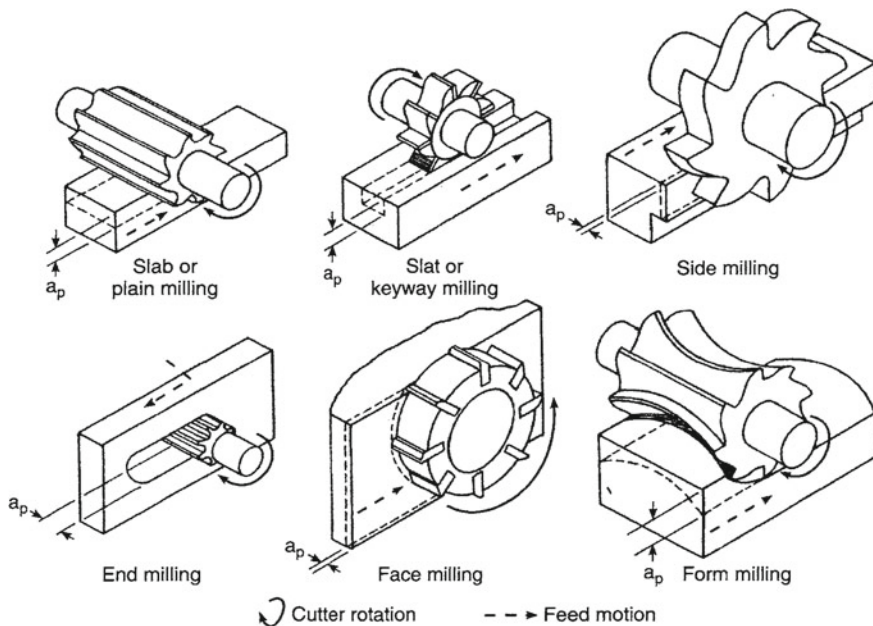


**Fig. 2.8** Types of cutters and milling operations (reprinted from Grzesik [5] with permission. © Elsevier)

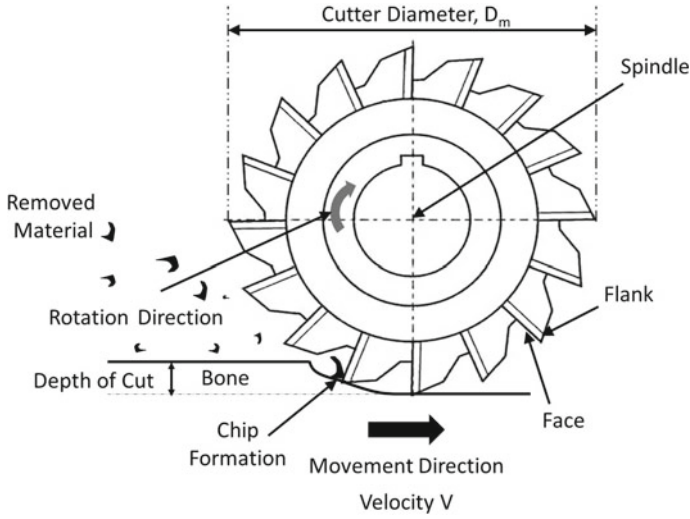


**Fig. 2.9** Schematic of milling cutter with essential elements

$$f_m = \frac{v_m}{N_m \cdot n} \quad (2.17)$$

where  $V_m$  is the machine feed rate (linear speed) of the workpiece and  $n$  is the number of teeth on the cutter periphery. Further, the milling time,  $t_m$  is expressed by the following equation.

$$t_m = \frac{l}{v_m} \quad (2.18)$$

where  $l$  is the length of the workpiece. Finally the material removal rate is given by

$$MRR_{mill} = \frac{lwd}{t_m} = wdv_m \quad (2.19)$$

where  $w$  is the width of the cut. Both power (Force  $\times$  Velocity) and torque (power/milling speed) requirements in milling are dependent on the forces (tangential, radial, and axial) acting on the cutter of multiple teeth and complex geometry and hence they are very difficult to calculate. However, they can be measured experimentally for a variety of conditions. Furthermore, for rapid milling, feed per tooth ( $f_m$ ) should be as high as possible. Such heavier feed, however is likely to exert greater load on the cutter teeth, workpiece, holding device, and milling machine. For a fragile material, a light feed is appropriate whereas a heavier feed is possible with soft materials. Irrespective of material type, a light feed leads to a good surface finish.

The various geometries such as flat surfaces, pockets, angles, contours, steps, and slots produced by milling are based on the following methods [1]. In slab milling or

peripheral milling, the axis of cutter rotation is parallel to the surface of the workpiece to be machined. Cutters used in slab milling possess straight or helical teeth and produce orthogonal or oblique sections. During this type of milling the operation can be conducted either as *up/conventional milling* or *climb/down milling* (Fig. 2.8). In up milling, the maximum chip thickness is at the end of the cut and hence tooth engagement is not a function of workpiece surface characteristics and the process is smooth. However, during the process the tool may chatter and the workpiece may need proper clamping to avoid its pulling upward. On the other hand, climb/down milling cutting starts with the thickest section of the chip and hence the downward component of cutting forces holds the workpiece in place. The surface characteristics influence the cutter teeth life during climb milling.

The milling process in which the cutter is mounted on a spindle with an axis of rotation perpendicular to the workpiece surface is called face milling (Fig. 2.8). During face milling, the cutter rotates at a rotational manner while the workpiece moves along a straight path in a linear manner. Like in slab milling, face milling operation can also be performed in up/conventional milling or climb/down milling mode. As the relative motion between the cutting teeth and the workpiece leaves feed marks on the machined surface during face milling, such surface roughness depends on insert corner geometry and feed per tooth. The method of *end milling* adopts the cutter with either sharp or tapered shank and rotates either on an axis perpendicular or tilted to the workpiece (Fig. 2.8). The end face of end mill with cutting teeth are used as a drill to start a cavity, whereas end mill with hemispherical ends produce curved surface and hollow end mill with internal cutting teeth machine the cylindrical surface of solid round workpiece. Other miscellaneous milling methods include straddle milling that is based on use of two or more cutters on an arbor to machine two parallel surfaces on the workpiece; and *form milling* to produce curved profiles using the cutters with specially shaped teeth.

## 2.5 Thermal Machining

A thermal machining using high energy density photon/electron heat sources such as laser, electron beam, and microwave is being extensively explored to machine various types of material systems [6, 7]. Although these techniques hold tremendous promise for machining various shapes, sizes, and materials they have not yet made inroads as routine commercial production techniques due to reasons such as but not limited to (1) lack of full understanding of interaction of these heat sources with material at atomic and molecular levels, (2) complexity and difficulty in maneuvering the heat source for delivery to workpiece during machining complex shapes, (3) lack of temperature dependent thermophysical properties of materials, and (4) safety issue with a reflected stray energy due to highly reflective nature of these intense heat sources with many types of materials. For all these prime and many other reasons, these thermal techniques are termed as non-traditional or un-conventional machining methods.

As these sources generate heat through interaction of the photons and electrons with the atoms and molecules in the surface and sub-surface regions of material. By controlling the intensity of incoming (input) high energy density photon/electron radiation, the temperature in heat source-material interaction region can be raised to the level to remove (machine) the material via melting or vaporization. The photonic/electronic radiation can be delivered in pulsed or continuous mode. The level (intensity or fluence) of energy delivered to the workpiece is function of power of the photon/electron source, traverse speed of photon/electron source or workpiece, photon/electron source coverage area on the workpiece surface, pulse frequency in case of pulse mode delivery, and photon/electron energy absorption characteristics with the workpiece surface. Based on these process parameters and thermo-physical properties of the workpiece material such as thermal conductivity, density, and specific heat as function of temperature, one can develop a computational heat transfer, mass transfer, and fluid flow based model to predict photon/electron energy required for the purpose of raising the temperature of material to remove (machine) it via melting or vaporization for a desired removal (machining) rate [8, 9]. Several two and three dimensional computational models incorporating various details for intense heat based material machining have been proposed in the open literature [8–36]. Due to the complexity associated with the interaction of materials with high energy photon/electron radiation and associated multi-physics phenomena along with lack of data in the open literature on temperature based thermos-physical properties of various materials, these computational models exist with various limitations in accurately predicting the temperatures and material removal rates. Nonetheless, they continue to provide important guidelines for future developments.

Considering the dynamic nature of the high energy density photon/electron radiation based machining with very short interaction times ranging from mili-to pico-seconds, it is extremely difficult to capture/realize various physical phenomena by in situ measurements of thermodynamic and kinetic parameters during machining process. In view of this, a multiphysics computational modeling approach incorporating physical phenomena such as heat transfer, fluid flow, convection mixing, surface tension, etc. remains the viable basis of computational efforts [8, 9]. Through understanding of correlations among these physical phenomena and in turn development of the correlation between these physical phenomena and processing parameters one can develop a better control on photon/electron energy based material removal (machining) rate and evolution of physical attributes (surface geometry and surface roughness) during machining operation. Furthermore, such methodology can be extended to optimization of the process to achieve higher machining efficiency.

During multidimensional high energy density photon/electron radiation based machining, material experiences various physical phenomena such as phase transition from solid-to-liquid-to-vaporization and material loss during evaporation. In addition, the material surrounding ablated region also experiences the transition dependent effects such as thermal expansion, melting, vaporization, along with generation of Marangoni convection in the melt and recoil pressure due to vaporization during heating as schematically presented in Fig. 2.10. These physical transitions are also associated with generation of various body and surface forces listed in Fig. 2.11

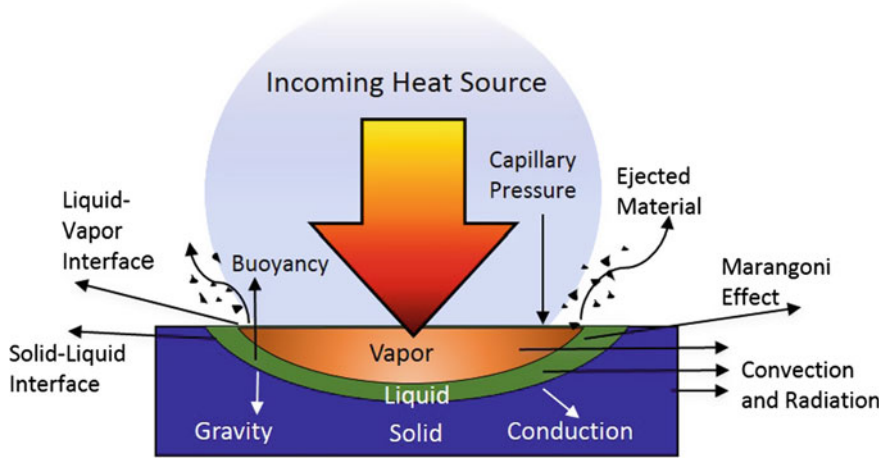


Fig. 2.10 Various physical phenomena within photon heat source-workpiece interaction region

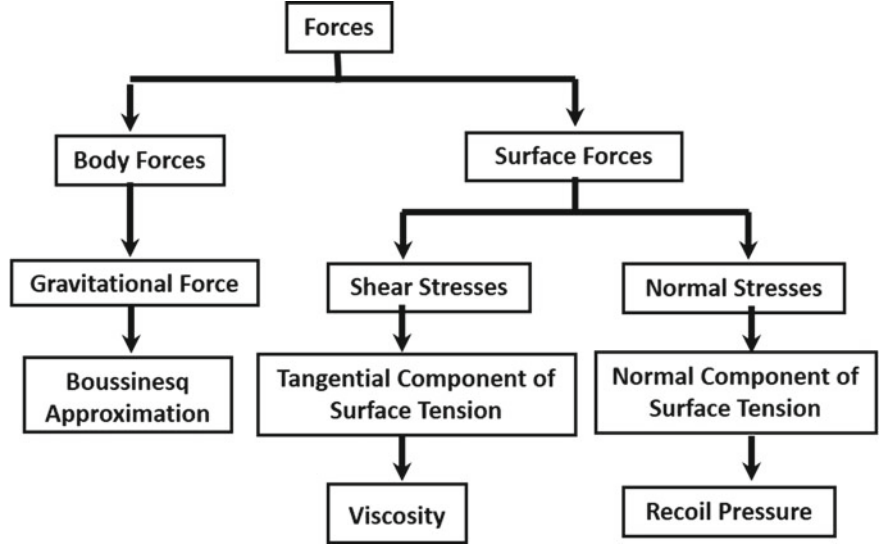


Fig. 2.11 Body and surface forces generated during thermal machining

[9] and depicted in Fig. 2.10. All these physical phenomena can be built into a complex computational model on the finite element platform. Such computational model based on the multiphysics approach can combine heat transfer, fluid flow, and structural mechanics for combinatorial effects of these physical phenomena. The model in turn can predict evolution of physical attributes/surface topography (depth, width, and geometry) of the machined region as schematically presented in Fig. 2.10 and corresponding machining rate.

The selective governing equations and boundary conditions for such multiphysics computational thermal models are presented below. As the material removal during such thermal machining is via controlled melting and vaporization, the prediction of temperature evolution is very important and can be determined by the solution of the equation governing the heat transfer given by

$$\rho C_p \left( \frac{\partial T}{\partial t} \right)_{(x,y,z)} = k \left[ \left( \frac{\partial T}{\partial x} \right)_{(y,z,t)} + \left( \frac{\partial T}{\partial y} \right)_{(x,z,t)} + \left( \frac{\partial T}{\partial z} \right)_{(x,y,t)} \right] \quad (2.20)$$

Here,  $k$  is the thermal conductivity,  $C_p$  is the specific heat and  $\rho$  is the density of the material. Of course, temperature variation will be dependent on many complex physical phenomena occurring during various times of the heat source-material interaction period. Hence, the accuracy of temperature predicted by solution to this fundamental equation depends upon how diligently one can conceive and incorporate them into the computational model. Further, the photon/electron heat source-workpiece interaction region is assigned a heat flux boundary with a moving photon/electron heat source or workpiece defined by

$$-k \left[ \frac{\partial T}{\partial x} + \frac{\partial T}{\partial y} + \frac{\partial T}{\partial z} \right] = PA + \epsilon \sigma [T^4 - T_0^4] + h[T - T_0] \quad (2.21)$$

Here,  $h$  is the heat transfer coefficient,  $\epsilon$  is the emissivity,  $P$  is the photon heat source power,  $A$  is the absorptivity,  $\sigma$  is Stefan-Boltzman constant, and  $T_0$  is the ambient temperature. All other surfaces are assigned convective cooling and surface to ambient radiation boundary conditions given by the following relationship

$$-k \left[ \frac{\partial T}{\partial x} + \frac{\partial T}{\partial y} + \frac{\partial T}{\partial z} \right] = \epsilon \sigma [T^4 - T_0^4] + h[T - T_0] \quad (2.22)$$

The heat transfer model can be extended to (1) multi-pass photon/electron heat source processing to account for the reheating effects and (2) multiphase and multicomponent nature of the workpiece by adopting a rule of mixture approach for thermophysical properties. Furthermore, a level-set method can be adopted to predict the evolution of solid-liquid-vapor interface. Temporal tracking of such interface predicts the volume melted and/or vaporized from the photon/electron heat source-workpiece interaction region and in turn assists in estimation of the geometrical dimensions (depth and width) of machined region and machining rate during heat source based machining. As stated earlier, the nature of formulation of computational model depends upon consideration to details and complexity of the process and hence, accordingly it is likely to provide the accurate values of machining attributes such as surface roughness and machining rate. These details can be found in several references in the open literature on computational modeling of heat source based machining [8–36].

The basic description and key aspects of all above fundamental operations of machining are summarized in Table 2.1. The table reveals the primary characteristics

**Table 2.1** Characteristics and key parameters of fundamental machining operations

Fundamental machining operation	Basic Description/characteristics	Key process aspects/parameters
Drilling	<ul style="list-style-type: none"> <li>• A process used to produce a hole</li> <li>• A process also can be extended to enlarge a hole and then called core or counter drilling</li> <li>• Utilizes a drill to accomplish the material removal</li> <li>• A drill is a rotary end cutting tool having one or more cutting lips with single or multiple helical or straight flutes for passage of chips and injection of cutting fluid</li> </ul>	<ul style="list-style-type: none"> <li>• Drill type—a drill with helical grooves or flutes</li> <li>• Geometric parameters of drill—point angle, lip-relief angle, a chisel-edge angle, and a helix angle</li> <li>• Drilling peripheral speed—high and low</li> <li>• Depth of cut/ depth of the hole generated</li> <li>• Feed: The rate that the drill advances into the material</li> <li>• Thrust: The axial force required to drill</li> <li>• Torque: The twisting moment required to drill</li> </ul>
Sawing	<ul style="list-style-type: none"> <li>• A cutting process to remove material by moving a blade in linearly reciprocating or unidirectional linear or circular motion</li> <li>• Sawing blade is a tool with series of small teeth on its periphery</li> <li>• Due to a narrow width of kerf a saw removes small volume of material</li> </ul>	<ul style="list-style-type: none"> <li>• Saw material—low alloy steel, high-carbon steel, stainless steel, and high speed steel</li> <li>• Saw shape—liner and circular</li> <li>• Saw pitch—tooth spacing</li> <li>• Saw tooth size</li> <li>• Saw tooth form—straight, raker, and wave</li> <li>• Saw tooth tip type—welded/fused/inserted diamond and ferrous or non-ferrous carbides</li> <li>• Saw tooth flank</li> <li>• Saw tooth back clearance angle</li> <li>• Saw tooth rake angle</li> <li>• Gullet depth</li> </ul>
Grinding/abrasive machining	<ul style="list-style-type: none"> <li>• A process of material removal via accelerated wear/fracture of the surface</li> <li>• A grinding tool comprises of a multitude of hard and angular hard abrasive grits bonded or not bonded to a substrate</li> </ul>	<ul style="list-style-type: none"> <li>• Grit type—conventional (aluminum oxide and silicon carbide) and super (cubic boron nitride and diamond) abrasives</li> <li>• Physical nature of grit—hardness, toughness, resistance to attrition and fracture, friability</li> </ul>

(continued)



**Table 2.1** (continued)

Fundamental machining operation	Basic description/characteristics	Key process aspects/parameters
	<ul style="list-style-type: none"> <li>• The material removal can be small fine or large scale</li> <li>• Typically abrasive/grinding machining is the last operation performed on the component to produce high quality surface finish tolerance</li> </ul>	<ul style="list-style-type: none"> <li>• Geometric nature of grit size and shape</li> <li>• Shape of grinding tool—disk, cylinder, cones and various geometric shapes</li> <li>• Grinding tool motion speed</li> </ul>
Milling	<ul style="list-style-type: none"> <li>• A machining operation to produce various surface geometries such a flat, pockets, angles, contours, steps, and slots</li> <li>• The machining action is generated by rotation of the tool and the feed by motion of the workpiece</li> <li>• The tools employed for milling have multiple teeth cutting edges configured around an axis that produce number of chips per revolution</li> </ul>	<ul style="list-style-type: none"> <li>• Type of milling tool—slab, face, end, straddle, slot/slit, angle, shell milling cutters</li> <li>• Milling tool rotary speed</li> <li>• Milling tool feed per tooth</li> <li>• Milling tool size</li> <li>• Maximum milling force, perpendicular and parallel to the milling direction</li> <li>• Axial Depth of cut</li> <li>• Number of end mill flutes</li> </ul>
Thermal machining	<ul style="list-style-type: none"> <li>• A machining operation involving removal of material by melting or vaporization</li> <li>• A machining tool can be an intense source of photonic beam of ultraviolet, infrared or microwave nature</li> <li>• The operation needs to be conducted in air or vacuum</li> <li>• Temperature required to remove material by melting or vaporization is generated through interaction of the photon source with the atoms or molecules of workpiece</li> <li>• Non-contact processes hence no mechanical stresses are involved</li> </ul>	<ul style="list-style-type: none"> <li>• Source of photon energy—laser, electron beam, microwave</li> <li>• Maneuverability of energy source—ability to focus/defocus, temporal and spatial distribution within and traverse speed of energy source</li> <li>• Power level of energy source</li> <li>• Operation mode of energy source—pulse and continuous</li> </ul>

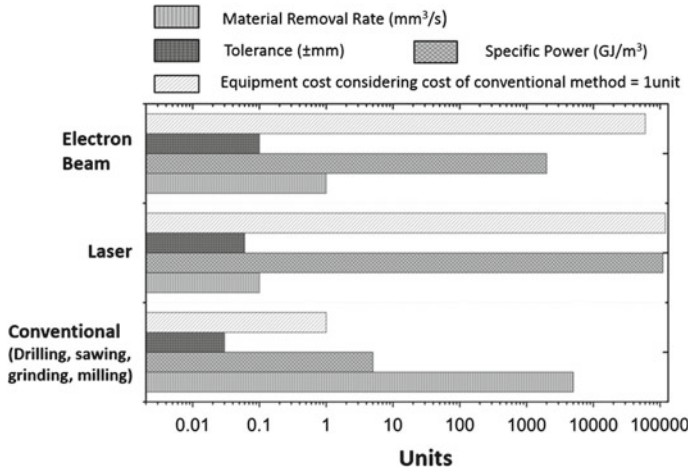


**Fig. 2.12** Comparison of machining attributes of various machining operations

and/or parameters of these operations and important parameter that influence the machining performance under these operating modes. Of course, all these operations are complex and dependent on complex nature of interactions among of these primary parameters and additional secondary parameters that are not included in Table 2.1. Furthermore, comparison of attributes of these machining operations/methods are presented on Fig. 2.12. Due to several recent advancements in development of industrial high power lasers, the new lasers are highly efficient in terms of energy delivery through fiber optic as well as integration of them with the complex motion systems. The machining operations with such integrated laser systems are highly efficient and can provide much better characteristics than what is listed in Fig. 2.12. Also costs of these efficient lasers have dropped down substantially and can cost less than \$100 K for 1 kW output power.

## 2.6 Machinability and Surface Quality

During all machining processes, the efficiency in terms of time and cost and desired outcome in terms of dimensions and surface finish of the process depend upon the machinability of a material that is being machined. In general, the machinability of a specific workpiece material can be expressed as the ease with which it can be machined which in turn can be rated in terms of surface finish of machined component, tool life, degree of dimensional control, machining force, and energy control which depends upon speed, depth, and feed [2, 37]. Although attempts have been made to rate machinability based on one or combinations of few above major factors,

due to the complex nature of any machining operation, establishing a quantitative relationship among these influencing factors to define a machinability for a specific material is difficult. This can further be complicated by the development and lack of control of temperature during machining. As a practical approach to this aspect, surface finish and tool life are considered prime factors in machinability.

In general, combination of good surface finish and integrity along with long tool life and requirement of low force and energy during machining are indication of good machinability. In metallic material systems, machinability ratings are based on comparing the machinability to AISI 1112 steel which is rated for its machinability at 100 or 1.0 [2, 37]. As there is no standard machinability rating for comparison available in non-metallic material systems, machinability rating of bones is difficult to find in the open literature. Furthermore, due to the multi-component nature in terms of chemical composition and physical architecture along with variation of these components as function of type (male and female) and age of the bone it is extremely difficult to quantify its machinability.

The surface quality produced during machining operation comprises of surface finish and surface integrity (physical and chemical properties). As stated above, resultant surface quality depends upon multiple factors such as machining force and energy control that in turn depend upon speed, depth, feed, and thermophysical and mechanical properties of the workpiece material [1]. Thus, controlling the machining process for desired surface quality is a complex and can be explored through experimental and computational efforts. The physical and chemical properties that affect the surface integrity are residual stresses, plastic deformation, fracture/cracking, and phase transformation. These physical and chemical properties affect mechanical (wear and fatigue) and corrosion/oxidation performances of machined workpiece. Apart from aesthetic appearance, surface finish directly and indirectly influences the physical and chemical performances of the machined workpiece.

The surface finish pertains to the geometric features of surface. According to the American National Standards Institute (ANSI), surface finish is defined with a set of standard terms such as profile, roughness, waviness, flaws, and lay. Profile is the contour of any section through a surface, roughness is relatively finely spaced surface irregularities, the spacing greater than roughness is waviness, and lay is the direction of the predominant surface pattern. The surface irregularities/imperfections occurring at infrequent interval and random locations are termed as flaws. These features are schematically illustrated in Fig. 2.13 [1]. According to ANSI/ASTM b46.1-1985 standard, surface roughness is quantitatively expressed as the arithmetic average,  $R_a$ , of deviation of the profile height (along the axis vertical to surface) increments from the centerline of the surface (Fig. 2.13b) and represented as follows.

$$R_a = \frac{1}{L} \int_{x=0}^{x=L} |y| dx \quad (2.23)$$

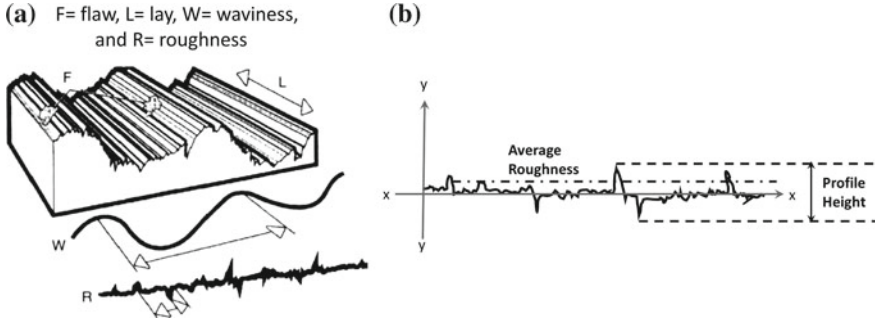


**Fig. 2.13** Schematic of features of surface roughness showing, **a** 3D view and **b** 2D cross section (reprinted from Grzesik [5] with permission. © Elsevier)

where  $L$  is the sampling length along the surface. This also can be expressed as

$$R_a = \frac{y_a + y_b + y_c + \dots + y_n}{n} \quad (2.24)$$

where surface profile heights at discrete locations  $a, b, c, \dots, n$  along the surface and number of locations (measurements) along the surface. Sometimes, roughness also can be expressed as the root mean square (rms),  $R_{rms}$ , the measurements from the centerline (Fig. 2.13b) given by the following equation.

$$R_{rms} = \left\{ \frac{\sum y_i^2}{n} \right\}^{\frac{1}{2}} \quad (2.25)$$

The range of surface roughness that can be achieved during these machining operations are presented in Fig. 2.14. Non-traditional applications are either the applications requiring very tight surface tolerances and high surface smoothness or the applications that can tolerate broad surface tolerances and rough surfaces. Also these conditions can be associated with machining of complex geometries and high volume and high production rate.

All above principles of machining of materials are recognized only for homogeneous material systems and do not take into account the material parameters such as multi-component (composite), multi-composition, and multi-phase nature along with the microstructural features such as grain size, grain shape, and grain distribution (uniform to multimodal). Even though these multiple features are likely to strongly influence the principles of machining and machining characteristics, they are often ignored due to the complex nature of the interactions between machine tool and multi-component/composition/phase material system. Hence, in spite of exploration or actual employment in real orthopaedic surgeries of these machining operations, their principles are not fully understood for machining of bones.

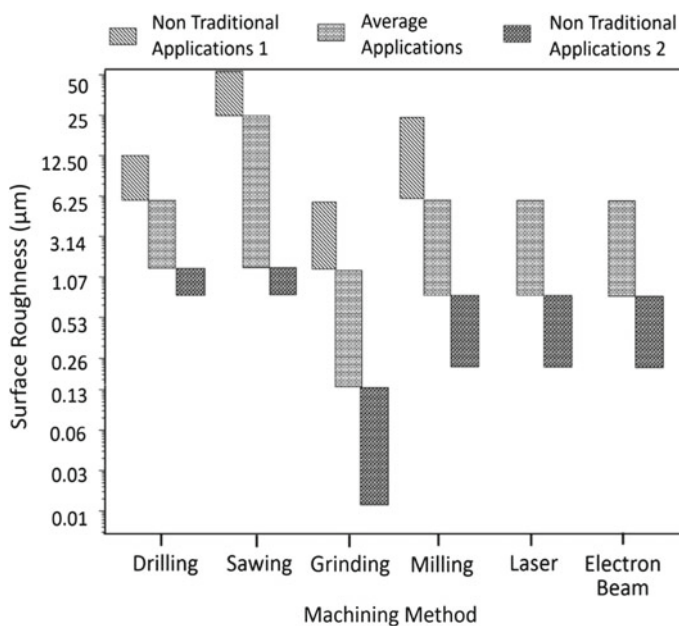


**Fig. 2.14** Surface roughness generated during various machining processes

Especially, in case of bone, this is more so due to its multi-component (hydrox-yapatite + cartilage + water), multi-composition (ceramic + organic + water), and multi-phase (solid + liquid) nature.

## References

1. J.E. Lee, Y. Rabin, O.B. Ozdoganlar, A new thermal model for bone drilling with applications to orthopaedic surgery. *Med. Eng. Phys.* **33**(10), 1234–1244 (2011)
2. S. Kalpakjian, S.R. Schmid, C.W. Kok, *Manufacturing Processes for Engineering Materials* (Pearson-Prentice Hall, Upper Saddle River, 2008)
3. J. Schey, *Introduction to Manufacturing Processes* (McGraw-Hill Book Co, New York, 1987)
4. V. Marinov, in *Manufacturing Technology* (2006), p. 74
5. W. Grzesik, *Advanced Machining Processes of Metallic Materials: Theory, Modeling and Applications* (Elsevier, Amsterdam, 2008)
6. N.B. Dahotre, A. Samant, *Laser Machining of Advanced Materials* (CRC Press, Boca Raton, Louisiana, 2011)
7. A.N. Samant, N.B. Dahotre, *J. Eur. Ceram. Soc.* **29**(6), 969 (2009)
8. A. Samant, *Laser machining of Structural Ceramics: Computational and Experimental Analysis*, PhD Thesis, University of Tennessee, USA (2009)
9. H.H. Vora, *Integrated Computational and Experimental Approach to Control physical Texture During Laser Machining of Structural Ceramics*, PhD Thesis, University of North Texas, USA (2013)
10. I. Tuersley, A. Jawaid, I. Pashby, *J. Mater. Process. Technol.* **42**(4), 377 (1994)

11. N.B. Dahotre, S. Harimkar, *Laser Fabrication and Machining of Materials* (Springer Science and Business Media, Berlin, 2008)
12. A. Kuar, B. Doloi, B. Bhattacharyya, *Int. J. Mach. Tools Manuf.* **46**(12), 1301 (2006)
13. A. Stournaras, K. Salonitis, P. Stavropoulos, G. Chryssolouris, in *Proceedings of the 10th CIRP International Workshop on Modeling of Machining Operations* (2007), pp. 549–553
14. A.N. Samant, N.B. Dahotre, *Ceram. Int.* **35**(5), 2093 (2009)
15. A.N. Samant, N.B. Dahotre, *Int. J. Mach. Tools Manuf.* **48**(12), 1345 (2008)
16. S. Lei, Y.C. Shin, F.P. Incropera, *J. Manuf. Sci. Eng.* **123**(4), 639 (2001)
17. J.C. Rozzi, F.E. Pfefferkorn, F.P. Incropera, Y.C. Shin, *Int. J. Heat Mass Transf.* **43**(8), 1409 (2000)
18. M.A. Moncayo, S. Santhanakrishnan, H.D. Vora, N.B. Dahotre, *Optics Laser Technol.* **48**, 570 (2013)
19. J.C. Rozzi, F.P. Incropera, Y.C. Shin, *Int. J. Heat Mass Transf.* **43**(8), 1425 (2000)
20. H.D. Vora, N.B. Dahotre, *Am. Ceram. Soc. Bull.* **92**, 4 (2013)
21. J.C. Rozzi, F.E. Pfefferkorn, F.P. Incropera, Y.C. Shin, *J. Heat Transfer* **120**(4), 899 (1998)
22. J.C. Rozzi, F.E. Pfefferkorn, F.P. Incropera, Y.C. Shin, *J. Heat Transfer* **120**(4), 907 (1998)
23. H.D. Vora, S. Santhanakrishnan, S.P. Harimkar, S.K. Boetcher, N.B. Dahotre, *J. Eur. Ceram. Soc.* **32**(16), 4205 (2012)
24. S. Lei, Y.C. Shin, F.P. Incropera, *Int. J. Mach. Tools Manuf.* **40**(15), 2213 (2000)
25. F. Quintero, F. Varas, J. Pou, F. Lusquiños, M. Boutinguiza, R. Soto, M. Pérez-Amor, *J. Phys. D: Appl. Phys.* **38**(4), 655 (2005)
26. H. Vora, N. Dahotre, *Int. J. Appl. Ceram. Technol.* **12**(3), 665 (2015)
27. M. Sussman, P. Smereka, S. Osher, *J. Comput. Phys.* **114**(1), 146 (1994)
28. H.D. Vora, S. Santhanakrishnan, S.P. Harimkar, S.K. Boetcher, N.B. Dahotre, *Int. J. Adv. Manuf. Technol.* **68**(1–4), 69 (2013)
29. N. Pierron, P. Sallamand, S. Matteï, in *Proceedings of the Comsol Multiphysics Conference* (2005)
30. H.D. Vora, N.B. Dahotre, *J. Manuf. Process.* **19**, 49 (2015). <http://dx.doi.org/10.1016/j.jmapro.2015.04.002>. <http://www.sciencedirect.com/science/article/pii/S1526612515000304>
31. S. Sun, M. Brandt, M. Dargusch, *Int. J. Mach. Tools Manuf.* **50**(8), 663 (2010)
32. H.D. Vora, N.B. Dahotre, *Lasers Manuf. Mater. Process.* **2**(1), 1 (2015)
33. M. Van Elsen, M. Baelmans, P. Mercelis, J.P. Kruth, *Int. J. Heat Mass Transf.* **50**(23), 4872 (2007)
34. A.N. Samant, N.B. Dahotre, *Int. J. Appl. Ceram. Technol.* **8**(1), 127 (2011)
35. S. Harimkar, A. Samant, A. Khangar, N.B. Dahotre, *J. Phys. D: Appl. Phys.* **39**(8), 1642 (2006)
36. Y. Yan, L. Li, K. Sezer, D. Whitehead, L. Ji, Y. Bao, Y. Jiang, *Int. J. Mach. Tools Manuf.* **51**(12), 859 (2011)
37. J. Beddoes, M. Bibby, *Principles of Metal Manufacturing Processes* (Butterworth-Heinemann, Burlington, Massachusetts, 1999)

Machining of Bone and Hard Tissues

Dahotre, N.; Joshi, S.

2016, VIII, 181 p. 164 illus., 62 illus. in color., Hardcover

ISBN: 978-3-319-39157-1